Shape and Structure of $N = Z$ ^{64}Ge: Electromagnetic Transition Rates from the Application of the Recoil Distance Method to a Knockout Reaction

K. Starosta,[1,2] A. Dewald,[3] A. Dunomes,[2] P. Adrich,[1] A. M. Amthor,[1,2] T. Baumann,[1] D. Bazin,[1] M. Bowen,[1,2] B. A. Brown,[1,2] A. Chester,[1,2] A. Gade,[1,2] D. Galaviz,[1] T. Glasmacher,[1,2] T. Ginter,[1] M. Hausmann,[1] M. Horoi,[4] J. Jolie,[3] B. Melon,[3] D. Miller,[1,2] V. Moeller,[1,2] R. P. Norris,[1,2] T. Pissulla,[3] M. Portillo,[1] W. Rother,[3] Y. Shimbara,[1] A. Stolz,[1] C. Vaman,[1] P. Voss,[1,2] D. Weisshaar,[1] and V. Zelevinsky[1,2]

[1]*National Superconducting Cyclotron Laboratory, Michigan State University, East Lansing, Michigan 48824, USA*
[2]*Department of Physics and Astronomy, Michigan State University, East Lansing, Michigan 48824, USA*
[3]*Institut für Kernphysik der Universtät zu Köln, D-50937 Köln, Germany*
[4]*Department of Physics, Central Michigan University, Mount Pleasant, Michigan 48859, USA*
(Received 13 March 2007; published 26 July 2007)

Transition rate measurements are reported for the 2_1^+ and 2_2^+ states in $N = Z$ ^{64}Ge. The experimental results are in excellent agreement with large-scale shell-model calculations applying the recently developed GXPF1A interactions. The measurement was done using the recoil distance method (RDM) and a unique combination of state-of-the-art instruments at the National Superconducting Cyclotron Laboratory (NSCL). States of interest were populated via an intermediate-energy single-neutron knockout reaction. RDM studies of knockout and fragmentation reaction products hold the promise of reaching far from stability and providing lifetime information for excited states in a wide range of nuclei.

DOI: 10.1103/PhysRevLett.99.042503 PACS numbers: 21.10.Tg, 21.60.Cs, 23.20.−g, 27.50.+e

Experiments involving $N = Z$ nuclei play a vital role in the understanding of nuclear structure. Along the $N = Z$ line, protons and neutrons occupy the same shell-model orbitals. The resulting overlap of nucleon wave functions leads to an amplification of the residual proton-neutron interactions. In nuclei with $28 < N = Z < 50$, large shell gaps open simultaneously for prolate and oblate quadrupole deformations [1]. Atomic nuclei in this region are the subject of vigorous experimental studies due to a remarkable diversity of shapes. Variations in the excitation energy of low-lying states in this region are often used to analyze the evolution of structure away from the doubly magic ^{56}Ni core. However, electromagnetic transition rates are recognized as providing a more sensitive probe of collectivity and deformation. The current Letter reports on the application of the recoil distance method (RDM) [2] to lifetime studies of $N = Z = 32$ ^{64}Ge.

Successful application of the RDM opens up new possibilities for lifetime measurements of excited nuclear states at fragmentation facilities. In the experiment reported here, states of interest were populated via an intermediate-energy single-neutron knockout from rare isotope beams of ^{65}Ge and ^{63}Zn. The measurement took advantage of state-of-the-art instruments available at the NSCL; it brought together the Coupled Cyclotron Facility [3] for acceleration of the primary beams, the A1900 mass separator for rare isotope selection [4], the diamond timing detector for particle identification of the incoming beam [5], the Segmented Germanium Array (SeGA) for γ-ray detection [6], the Köln/NSCL plunger device for the RDM [7], and the high-resolution S800 spectrograph for identification of the reaction products [8]. This unique combination offers access to a wide range of exotic nuclei which can be investigated via the RDM for lifetime information. Such studies can provide information on transition rates far from the line of stability.

Ground-state shapes in $28 < N = Z < 50$ nuclei are predicted to evolve from spherical to triaxial, oblate, prolate, and back to spherical as mass increases [1] due to occupation of identical deformation-driving orbitals. Moreover, excited levels can have significantly different structure than the ground state. Currently, the reduced transition probabilities $B(E2, 2_1^+ \rightarrow 0_1^+)$ in even-even $N = Z$ nuclei beyond doubly magic ^{56}Ni are known only in ^{72}Kr from a recent Coulomb excitation experiment [9]. While the single-step Coulomb excitation process is used very effectively to investigate transition rates to the first excited state [10], the RDM combined with knockout or fragmentation reactions provides an opportunity to access states beyond the 2_1^+. In particular, the lifetime of the 2_1^+ and 2_2^+ states in ^{64}Ge, where an instability to quadrupole triaxial deformation is predicted from microscopic models [11], is reported below.

The reduced $E2$ transition rates measured here for the 2_1^+ and 2_2^+ states in ^{65}Ge are in excellent agreement with the large-scale shell-model calculations which use the recently developed GXPF1A effective Hamiltonian [12] exploited in a study of energy levels in ^{56}Ni [13]. GXPF1A was derived from a microscopic calculation by Hjorth-Jensen based on renormalized G-matrix theory with the Bonn-C interaction [14], and was refined by a systematic fitting of the important linear combinations of two-body matrix elements to low-lying states in nuclei from $A = 47$ to $A = 66$, including some states of ^{56}Ni [12,15]. The GXPF1A results yield spectroscopic quadrupole moments of nearly equal magnitude but opposite sign for the 2_1^+ and 2_2^+ states

 © 2007 The American Physical Society

in ^{64}Ge which can be understood from an anharmonicity in collective vibrations.

In the current experiment the RDM developed for intermediate-energy Coulomb excitation [2] was successfully applied in a measurement of nuclear states populated in single-neutron knockout reactions. A cocktail beam of rare isotopes comprised of 5% ^{65}Ge, 35% ^{64}Ga, 52% ^{63}Zn, and 8% ^{62}Cu was produced via in-flight projectile fragmentation of ^{78}Kr at 150 MeV/u as described in [16]. The constituents of the incoming beam were identified on an event-by-event basis from the rf time of flight between the K1200 cyclotron and the timing diamond detector [5] in the object of the S800 spectrograph [8]. The use of the radiation hard diamond for particle identification was crucial to handle the $\sim 10^6$ particle-per-second rate of the incoming beam. The quality of the identification was sufficient to completely separate incoming beam components in the offline analysis.

The nuclei of interest for the current study were produced in nuclear reactions at the target-degrader position of the Köln/NSCL plunger device [7]. The plunger device was mounted at the target position of the S800 spectrograph [8]. The mass and charge of the reaction products were extracted on an event-by-event basis from the time-of-flight and energy-loss information. The time of flight was measured between the diamond detector in the object of the S800 and the $E1$ plastic scintillator in the S800 focal plane. The energy-loss measurement was performed in the ionization chamber at the S800 focal plane [17]. In the offline analysis the outgoing reaction products were identified separately for each component of the incoming cocktail beam. Below, two channels are discussed: the single-neutron knockout from ^{63}Zn leading to ^{62}Zn and from ^{65}Ge leading to ^{64}Ge. The transition rates in ^{62}Zn are known from measurements in stable beam facilities [18] and serve here as a consistency check.

The reaction products emerged from the 500 μm thick ^{nat}C plunger target with a velocity of $\beta_H \sim 0.39$. A stationary 250 μm thick ^{93}Nb degrader positioned downstream of the target further reduced the velocity to $\beta_L \sim 0.35$. Depending on whether the decay occurred in flight between the target and the degrader or after slowing down in the degrader, the γ rays exhibit different Doppler shifts. Consequently, the γ-ray spectra contain two peaks for each transition. The lifetime of the state can be inferred from relative intensities of the peaks as a function of target-degrader separation using the information on the ion velocity contained in the Doppler shift.

The Doppler-shifted γ rays were recorded by the Segmented Germanium Array [6] with two rings of 7 and 8 detectors at a laboratory angle of 30° and 140°, respectively. The data were recorded for target-degrader separations of 0, 200, and 500 μm. In addition, a run without the degrader was performed to measure the velocity of the reaction products downstream from the target. This run also provided information on the relative population of excited states from the reaction of interest.

The lifetimes under investigation are comparable with the times needed to cross the plunger target/degrader. Thus, the RDM analysis described in Ref. [2] was modified so that the measured lifetimes were extracted from a least square fitting between the calculated and the experimentally observed line shape of gamma-ray transitions. The quality of the best fits is illustrated in Fig. 1.

While the details of the above analysis will be presented in a separate paper, it is worthwhile to stress a few aspects of the procedure here. The parameters which define the line shape for a given target-degrader separation, with the exception of the lifetime, are the velocities of the nuclei of interest at the moment of the gamma emission and the geometrical dimension and energy resolution of the Ge detectors in use. In the current experiment the information on the velocities of the incoming beam ions and the corresponding outgoing reaction products are defined within 2% and 6% by the settings of the A1900 and the S800 separators, respectively. Only very small modifications of the calculated stopping powers were needed to reproduce the measured values.

The response of the SeGA array is understood from the offline source calibrations and Lorentz transformation

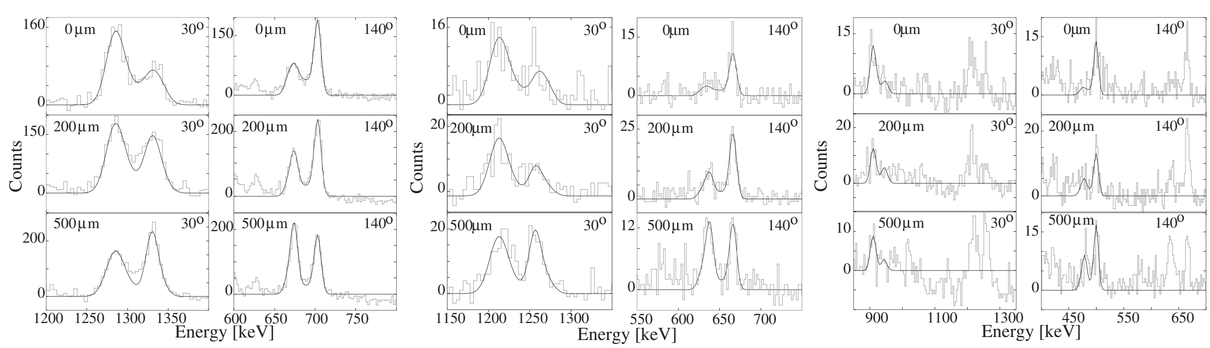

FIG. 1. Experimental data and line-shape fits for the 954-keV $2_1^+ \rightarrow 0_1^+$ transition in ^{62}Zn (left), 901-keV $2_1^+ \rightarrow 0_1^+$ transition in ^{64}Ge (middle), and 677-keV $2_2^+ \rightarrow 2_1^+$ transition in ^{64}Ge (right). In each panel the left/right spectra are for the SeGA rings at 30°/140°, while top, middle, and bottom spectra are for 0, 200, and 500 μm target-degrader separations, respectively. The Doppler corrections account for the detector segmentation but not for the angular position of the detector in the array. See text for further details on line-shape calculations.

from the source to the laboratory reference frame. The energy and angular straggling of the reaction products as well as the energy resolution of the gamma detectors are described by a single parameter which enters as a width parameter into Gaussian functions out of which the line shape is composed. In the present analysis, four different width-parameter values were used corresponding to decays occurring in or after the target and for the observation of the gamma transitions in the 30° or 140° Ge ring of the SeGA array. These values were selected to give a good representation of the width of the two components of gamma-ray transitions observed in the spectra including those measured with the plunger target only.

In plunger experiments at intermediate energies the beam has enough energy to react in the degrader; here 40% of the excitations came from these reactions, as determined from the line-shape analysis. The same fraction of reaction on the degrader resulted from fits for ^{64}Ge and for ^{62}Zn. Thus, having fixed the line-shape parameters, the level lifetimes were deduced from a fit of the calculated line shapes to the measured spectra; the only free parameters of the fit were the lifetimes of interest and normalization factors to account for different statistics accumulated at different target-degrader distances and observation angles. Small variations of all fit parameters from the optimal values were studied for error analysis.

For ^{62}Zn the 2_1^+ lifetime was determined by taking into account the 10% feeding from the 2_2^+ state with the 3.8(6) ps lifetime given in the literature [18]. The extracted lifetime of 4.2(7) ps is in excellent agreement with the 4.2(3) ps lifetime of Ref. [18]. Separate studies of the unobserved feeding indicate that ~90% of the intensity of the 2_1^+ decay in ^{62}Zn comes from fast feeding. This observation makes the knockout reaction an excellent tool for lifetime measurements.

In ^{64}Ge a significant feeding of ~30% via the 677-keV transition from the 2_2^+ to the 2_1^+ level was observed, see Fig. 1. Thus, the lifetime of the 2_2^+ state was fitted to the data shown in Fig. 1 utilizing a single exponential decay, while the corresponding fit for the 2_1^+ state was done taking into account the observed feeding. The results for the first measurements of the 2_1^+ and 2_2^+ state lifetimes of the $N = Z$ ^{64}Ge are 3.3(5) and 8^{+4}_{-2} ps, respectively.

From the measured lifetimes and data in Refs. [18,19], experimental observables were extracted and compared to the shell-model GXPF1A calculations as summarized in Table I. The GXPF1A interaction was recently used [13] to describe the low-lying states and the first rotational band of ^{56}Ni, by considering 16 valence particles in the pf model space (^{64}Ge is described by 16 valence holes). Reference [20] suggests that the contribution of the $g_{9/2}$ orbital may be small in Zn and Ge, while the Nilsson diagram suggests that the contribution of the $f_{7/2}$ orbital may be important in this region. The canonical effective charges of $e_p = 1.5e$ and $e_n = 0.5e$ were used for the $B(E2)$ calculations. It should be stressed that the agreement between calculated and observed excitation energies for ^{64}Ge is better than 50 keV, while the transition rates are reproduced within the experimental errors, except for the weak $2_2^+ \rightarrow 0_1^+$ transition. A similar level of agreement is reached for ^{62}Zn. In both cases, the theory predicts a negative and positive quadrupole moment for the 2_1^+ and the 2_2^+ states, respectively.

TABLE I. Comparison between the experimental data and the GXPF1A shell-model calculations for ^{64}Ge and ^{62}Zn.

Nucleus	Observable	Experiment	Theory	Unit
^{64}Ge	$E(2_1^+)$	0.902	0.938	MeV
^{64}Ge	$E(0_2^+)$		1.353	MeV
^{64}Ge	$E(2_2^+)$	1.579	1.559	MeV
^{64}Ge	$E(4_1^+)$	2.053	1.995	MeV
^{64}Ge	$B(E2, 2_1^+ \rightarrow 0_1^+)$	410(60)	406	e^2 fm^4
^{64}Ge	$B(E2, 2_2^+ \rightarrow 2_1^+)$	620(210)	610	e^2 fm^4
^{64}Ge	$B(E2, 2_2^+ \rightarrow 0_1^+)$	1.5(5)	14	e^2 fm^4
^{64}Ge	$B(E2, 0_2^+ \rightarrow 2_1^+)$		483	e^2 fm^4
^{64}Ge	$B(E2, 0_2^+ \rightarrow 2_2^+)$		12	e^2 fm^4
^{64}Ge	$B(E2, 4_1^+ \rightarrow 2_1^+)$		674	e^2 fm^4
^{64}Ge	$B(E2, 4_1^+ \rightarrow 2_2^+)$		9	e^2 fm^4
^{64}Ge	$Q(2_1^+)$		−18.6	e fm^2
^{64}Ge	$Q(2_2^+)$		+18.5	e fm^2
^{62}Zn	$E(2_1^+)$	0.954	1.012	MeV
^{62}Zn	$E(2_2^+)$	1.805	1.908	MeV
^{62}Zn	$B(E2, 2_1^+ \rightarrow 0_1^+)$	250(18)	295	e^2 fm^4
^{62}Zn	$B(E2, 2_2^+ \rightarrow 2_1^+)$	290(50)	231	e^2 fm^4
^{62}Zn	$B(E2, 2_2^+ \rightarrow 0_1^+)$	4.5(7)	11	e^2 fm^4
^{62}Zn	$Q(2_1^+)$		−22.3	e fm^2
^{62}Zn	$Q(2_2^+)$		+13.8	e fm^2

The opposite quadrupole moments can be qualitatively explained by large-amplitude collective dynamics. In the case of an anharmonic vibrator Hamiltonian, which seems applicable based on the observed excitation energy pattern and from microscopic calculations of Ref. [20], the most important anharmonicity is quartic (α^4) in the quadrupole coordinate (α). The semimicroscopic estimates of various types of anharmonicity were given in [21] based on the soft quadrupole mode with low quadrupole frequency, relatively close to the RPA instability. Here the quadrupole frequency is $\sim 1/2$ of the pairing gap, i.e., not very low. In the limiting case of strong quartic anharmonicity, the prediction [22,23] is $R = E(4_1)/E(2_1) = 2.09$. The perfect case is ^{100}Pd, where all states of the yrast band practically coincide with predictions of strong quartic anharmonicity that is characterized by O(5) symmetry. In the case of ^{64}Ge $R = 2.13$, close to this limit are ^{70,72}Ge with $R = 2.07$.

The cubic anharmonicity, discussed first in Ref. [24], is related to single-particle levels changing with deformation; this can give a first order phase transition to static deformation. In the limiting case of strong quartic anharmonicity, the cubic term is typically small. This is analogous to the three-phonon vertex in quantum electrodynamics that is strictly forbidden by the Furry theorem (virtual contributions of electrons and positrons cancel exactly). For $N = Z$ nuclei this would be the case for exact particle-hole symmetry; in the BCS theory the effect is proportional to the sum of contributions $(u^2 - v^2)$ which almost cancel, but not exactly. It can be observed from a Nilsson diagram that for ^{64}Ge the lowest energy states which originate from the $g_{9/2}$ orbital go down for both signs of deformation, while the hole level originating from the $f_{7/2}$ orbital goes up on the prolate side [25]. With a large amplitude of zero point quadrupole motion, the nucleons probe all these shapes, and the cubic anharmonicity is relatively important. Moreover, it should be stressed that the effect is enhanced by the coherent action of protons and neutrons occupying the same shells. The cubic anharmonic term mixes the states with phonon numbers differing by one unit (its contribution to energy comes only in the second order and therefore is not large). For the 2_1^+ and the 2_2^+ states this mixing results in quadrupole moments equal in magnitude and opposite in sign as given in Table I.

If the amplitude of zero point vibration is large and various deformations are probed, there appears "virtual rotation" [23] based on slowly evolving dynamic deformation. This splits the two-phonon states by $\frac{1}{2J} \times I(I+1)$, for ^{64}Ge $\frac{1}{2J} = 31$ MeV. For good rotors the "Alaga ratio" of the absolute value of the quadrupole moment in the lowest 2^+ state to the $\sqrt{B(E2)}$ from this state to the ground state is $2/7$. Here we have instead 0.9, which means that the transition probabilities are much weaker than it would be for a good rotor.

Previous studies of ^{64}Ge [11] and microscopic calculations therein indicate that this nucleus is unstable with respect to quadrupole triaxial deformation in the ground state. There, the experimental information on triaxiality as measured by Bohr's parameter γ is inferred from a comparison of the collective model predictions with the energies of low-lying 2^+ states and the ratio of $B(E2, 2_2^+ \to 2_1^+)/B(E2, 2_1^+ \to 0_1^+)$. While the absolute transition rates reported herein are consistent with the triaxial rigid rotor model of $\beta \sim 0.265$ $\gamma \sim 27°$ we agree with the conclusions of Ref. [11] that γ shape fluctuations are important to explain the transition rates and observed pattern of low energy levels simultaneously.

In summary, picosecond RDM lifetime measurements were performed using a unique combination of state-of-the-art instruments and knockout reactions with rare isotope beams at the NSCL. Studies of this type hold the promise of reaching far from stability and providing lifetime information for intermediate-spin excited states in a wide range of nuclei. The absolute $E2$ transition rates measured here for the 2_1^+ and 2_2^+ states in $N = Z$ ^{64}Ge are in excellent agreement with state-of-the-art large-scale shell-model calculations.

This work is supported by the US NSF under Grants No. PHY-0606007, No. PHY-0555366 and MRI PHY-0619497, US DOE under Grant No. DE-FC02-07ER41457, and also partly by the DFG (Germany) under Contract No. DE1516/-1 and GSI, F.u.E. Contract No. OK/JOL. The authors acknowledge computational resources provided by the MSU High Performance Computing Center and by the Center of High Performance Scientific Computing at Central Michigan University.

[1] Nazarewicz *et al.*, Nucl. Phys. **A435**, 397 (1985).
[2] A. Chester *et al.*, Nucl. Instrum. Methods Phys. Res., Sect. A **562**, 230 (2006).
[3] P. Miller *et al.*, *Proceedings of the 2001 Particle Accelerator Conference, Chicago, IL*, edited by P. Lucas (IEEE, Piscataway, NJ, 2001), p. 2557.
[4] D. J. Morrissey *et al.*, Nucl. Instrum. Methods Phys. Res., Sect. B **204**, 90 (2003).
[5] A. Stolz *et al.*, Diam. Relat. Mater. **15**, 807 (2006).
[6] W. F. Mueller *et al.*, Nucl. Instrum. Methods Phys. Res., Sect. A **466**, 492 (2001).
[7] A. Dewald *et al.*, GSI Scientific Report 2005, p. 38 (2006).
[8] D. Bazin *et al.*, Nucl. Instrum. Methods Phys. Res., Sect. B **204**, 629 (2003).
[9] A. Gade *et al.*, Phys. Rev. Lett. **95**, 022502 (2005); **96**, 189901(E) (2006).
[10] J. M. Cook, T. Glasmacher, and A. Gade, Phys. Rev. C **73**, 024315 (2006).
[11] P. J. Ennis *et al.*, Nucl. Phys. **A535**, 392 (1991).
[12] M. Honma, T. Otsuka, B. A. Brown, and T. Mizusaki, Eur. Phys. J. A **25**, 499 (2005).
[13] M. Horoi, B. A. Brown, T. Otsuka, M. Honma, and T. Mizusaki, Phys. Rev. C **73**, 061305(R) (2006).
[14] M. Hjorth-Jensen, T. T. S. Kuo, and E. Osnes, Phys. Rep. **261**, 125 (1995).
[15] M. Honma, T. Otsuka, B. A. Brown, and T. Mizusaki, Phys. Rev. C **69**, 034335 (2004).
[16] A. Stolz *et al.*, Nucl. Instrum. Methods Phys. Res., Sect. B **241**, 858 (2005).
[17] J. Yurkon *et al.*, Nucl. Instrum. Methods Phys. Res., Sect. A **422**, 291 (1999).
[18] H. Junde and B. Singh, Nuclear Data Sheets **91**, 317 (2000).
[19] B. Singh, Nuclear Data Sheets **78**, 395 (1996).
[20] K. Kaneko, M. Hasegawa, and T. Mizusaki, Phys. Rev. C **70**, 051301(R) (2004).
[21] V. G. Zelevinsky, Int. J. Mod. Phys. E **2**, 273 (1993).
[22] O. K. Vorov and V. G. Zelevinsky, Yad. Fiz. **37**, 1392 (1983) [Sov. J. Nucl. Phys. **37**, 830 (1983)].
[23] O. K. Vorov and V. G. Zelevinsky, Nucl. Phys. **A439**, 207 (1985).
[24] D. M. Brink, A. F. R. De Toledo Piza, and A. K. Kerman, Phys. Lett. **19**, 413 (1965).
[25] For that reason the $f_{7/2}$ state has to be included in the shell-model space.